3D homogenization: identification of equivalent anisotropic material properties of heterogeneous structures and dynamic application on preloaded finite element models and superelements

P. Millithaler[1,2]**, É. Sadoulet-Reboul**[2]**, M. Ouisse**[2]**, J.-B. Dupont**[1]**, N. Bouhaddi**[2]

[1] Vibratec, 28 chemin du petit bois, BP36, F-69131 Écully Cedex, France,
e-mail: **pierre.millithaler@vibratec.fr**

[2] Femto-S.T. Institute, UMR CNRS 6174 24 chemin de l'Épitaphe, 25000 Besançon, France

Abstract

Although several mature approaches and theories exist for the analysis of 2D-heterogeneous finite element models, few have been developed for computing equivalent models to 3D-heterogeneous structures. Yet, the cases of equivalent modelling of anisotropic or preconstrained structures are hardly ever discussed in the literature. In this paper, a novel method of equivalent material identification is proposed for finite element anisotropic structures and for models subjected to preloads, with high computation speed and low resource requirements. The proposed approach is applied to superelements and enables converting a stiffness matrix into the equivalent material's elasticity matrix. Applied to preloaded homogeneous and heterogeneous finite element structures, the method leads to equivalent models. Compared at low frequencies, the dynamic behaviour of each of the preloaded structures and its corresponding equivalent are in good accordance.

1   Introduction

Frequently used in the domain of composite structures, a large number of so-called "homogenization" methods exist in order to model 2D-heterogeneous structures such as laminates or honeycomb plates. Some of the most common ones have been thoroughly reviewed in [1]. The large majority of these techniques are applied to structures whose global behaviours are orthotropic, therefore defined by 9 explicit elastic coefficients; Young's moduli E_x, E_y and E_z, shear moduli G_{xy}, G_{yz} and G_{zx} and Poisson's coefficients ν_{xy}, ν_{yz} and ν_{zx} when considering the directions x, y and z. Relatively few amongst them are both accurate and simple to implement in the case of 3D structures, and seldom lead to equivalent elasticity matrices.

There yet exists some situations in which orthotropic materials are not accurate enough to model the behaviour of a given heterogeneous structure. In such cases, equivalent materials are called anisotropic (or sometimes "triclinic") and need to be defined by their most general expression. Instead of 9 explicit elastic coefficients, anisotropic materials are defined by 21 independent constants [2] composing the elasticity matrix C in Hooke's law $\{\sigma\} = C\{\varepsilon\}$, where $\{\sigma\}$ is the stress tensor and $\{\varepsilon\}$ the strain tensor [3]. The entire linear system is detailed as following:

$$
\begin{Bmatrix} \sigma_{11} \\ \sigma_{22} \\ \sigma_{33} \\ \sigma_{23} \\ \sigma_{13} \\ \sigma_{12} \end{Bmatrix} = \begin{bmatrix} c_{11} & c_{12} & c_{13} & c_{14} & c_{15} & c_{16} \\ & c_{22} & c_{23} & c_{24} & c_{25} & c_{26} \\ & & c_{33} & c_{34} & c_{35} & c_{36} \\ & & & c_{44} & c_{45} & c_{46} \\ & \text{sym.} & & & c_{55} & c_{56} \\ & & & & & c_{66} \end{bmatrix} \begin{Bmatrix} \varepsilon_{11} \\ \varepsilon_{22} \\ \varepsilon_{33} \\ 2 \cdot \varepsilon_{23} \\ 2 \cdot \varepsilon_{13} \\ 2 \cdot \varepsilon_{12} \end{Bmatrix}, \tag{1}
$$

where the indices 1, 2 and 3 respectively refer to the directions x, y and z.

Although their formulations are not straightforward to implement for finite element models, an analytical homogenization method that can be applied to 3D triclinic structures has been developed in [4], the core of which was taken as a reference for other approaches. Leading to equivalent elasticity matrices, it nonetheless fails to model external effects onto the structure, such as friction or preconstraining conditions.

Several other works such as [5], [6], [7] or [8] have addressed the issues of modelling friction or heterogeneity with equivalent properties, but none enables computing equivalent elasticity matrices, though necessary for creating finite element models and updating procedures. As for superelements and preconstrained structures, there does not exist to the author's knowledge any approaches capable of determining equivalent homogeneous elasticity matrices in such cases.

This is why a new method is proposed, in order to create homogeneous materials whose elasticity matrices approximate the phenomena existing in the initial heterogeneous structures, take into account boundary conditions and external loadings as well.

In the following sections, the development of the algorithm for the identification of elastic properties in the case of triclinic materials will be presented, and followed by applications on numerical structures.

2 Identification method for anisotropic materials

Orthotropic material properties imply no couplings between tension-compression and shear. When modelling a heterogeneous assembly or a structure subjected to preloads or contact effects with equivalent homogeneous materials, these no-coupling assumptions may not be valid in the general case, and any linear elasticity matrix approximating the global behaviour shall be therefore expressed as anisotropic, or "triclinic". Representing non-linear phenomena by linear elasticity matrices is therefore an approximation of the real behaviour. Entire elasticity matrices (see Hooke's law in Equation (1)), therefore describe the equivalent material properties, and are identified by the means of finite element models.

2.1 Computation of the stiffness matrix

The example taken for the development of the method is a finite element model made of two 8-node solid elements, as shown on Figure 1: the elements <1, 2, 3, 4, 101, 102, 103, 104> and <105, 106, 107, 108, 5, 6, 7, 8> are superimposed along the z-axis, and preloads are applied onto the structure (red arrows). In order to model possible friction properties, the two elements have to be separated: the interface nodes are doubled and coincident (as illustrated in the ellipses on Figure 1), and each of them only belongs to one of the two elements. If no friction conditions are to be taken into account, the interface nodes may be merged and therefore linked to both of the elements. The dimensions of the assembled cuboid are L_x, L_y and L_z, and its faces' respective areas A_x (faces $x = 0$ and $x = 1$), A_y (faces $y = 0$ and $y = 1$) and A_z (faces $z = 0$ and $z = 1$).
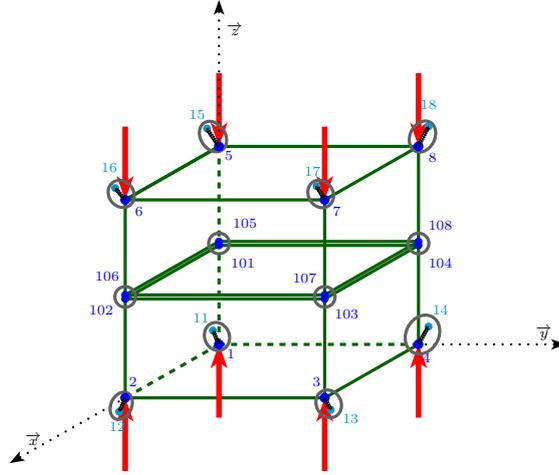
Figure 1: Finite element sample

In order to stabilise the system, each of the outer nodes 1, 2, 3, 4, 5, 6, 7 and 8 is linked to a node-to-ground 3D-stiffness element (this is represented equivalently by a coincident, clamped node and a 3D-stiffness linking element). The numerical values of these stiffness elements have to be small enough not to perturb the entire structure's stiffness matrix values. Now, the preloads $\overrightarrow{\sigma_0}$ and $\overrightarrow{\sigma_1}$ applied to the system can be expressed with

$$\overrightarrow{\sigma_0} = \frac{1}{A_z} \sum_{i \in \mathcal{U}_{z0}} F_i \cdot \overrightarrow{z} \tag{2}$$

and

$$\overrightarrow{\sigma_1} = -\frac{1}{A_z} \sum_{i \in \mathcal{U}_{z1}} F_i \cdot \overrightarrow{z} \ , \tag{3}$$

where the values F_i stand for the loadings at the nodes 1 through 8, and where the sets of nodes $\mathcal{U}_{x0}, \mathcal{U}_{x1}, \mathcal{U}_{y0}, \mathcal{U}_{y1}, \mathcal{U}_{z0}$ and $\mathcal{U}_{z1}$ are detailed in the Appendix, in Table 4. The contact properties are defined according to the physics of the interface (deformable bodies, friction, etc.). Creating the superelement (with translational degrees of freedom) at the outer nodes is an efficient way to output a stiffness matrix, but the solver used has to take into account the influence of the preloads and the contact properties on the values.

2.2 Determination of the elastic properties

As it has been shown, the 21 independent coefficients of a triclinic elasticity matrix C have to be identified. To do this, the proposed approach consists in computing the compliance matrix S such that $S = C^{-1}$. The general relation of Hooke's law, detailed in Equation (1), is reversed to express the matrix S:

$$\begin{Bmatrix} \varepsilon_{xx} \\ \varepsilon_{yy} \\ \varepsilon_{zz} \\ 2 \cdot \varepsilon_{yz} \\ 2 \cdot \varepsilon_{zx} \\ 2 \cdot \varepsilon_{xy} \end{Bmatrix} = \begin{bmatrix} S_{11} & S_{12} & S_{13} & S_{14} & S_{15} & S_{16} \\ & S_{22} & S_{23} & S_{24} & S_{25} & S_{26} \\ & & S_{33} & S_{34} & S_{35} & S_{36} \\ & & & S_{44} & S_{45} & S_{46} \\ & \text{sym.} & & & S_{55} & S_{56} \\ & & & & & S_{66} \end{bmatrix} \begin{Bmatrix} \sigma_{xx} \\ \sigma_{yy} \\ \sigma_{zz} \\ \sigma_{yz} \\ \sigma_{zx} \\ \sigma_{xy} \end{Bmatrix}. \tag{4}$$

To calculate all the constants of S, the method needs six series of simulations, ie. one per component of $\{\varepsilon\}$. Thus, for each series i, one has to perform as many independent simulations as the corresponding line's constants S_{ij}. The first series of simulations are pure tension schemes. The example of series xx (corresponding to the deformed state ε_{xx}) is made by a displacement δ_x enforced along $+x$ to the nodes of the face $x = 1$, the same displacement δ_x enforced along $-x$ to the nodes of the face $x = 0$, and constraints of plane contact applied to the face $x = 0$ and $z = 0$. This is illustrated on Figure 2.
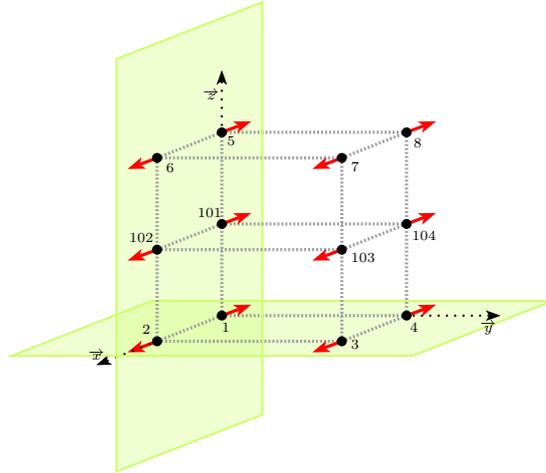

Figure 2: Pure tension along x

Computing the stress values σ_{ij} therefore leads to the constants S_{ij} for each of the schemes xx, yy and zz. In a similar way, the terms of S involving shear are computed by simulations of shear. Yet in the cases of heterogeneous structures, some attention must be paid for defining shear. Although the moduli are often defined without respect for either sliding or transverse shear configurations (both are equivalent in the theory of homogeneous structures [9, 10, 2, 11]), it may be observed in practice that the two behaviours are not equivalent in general when homogenizing heterogeneous structures. This is why in this paper, the analysis separates sliding shear (illustrated on Figure 3a) from transverse shear (illustrated on Figure 3b), in the respective "**T1**" and "**T2**" methods, which are yet completely identical for the determination of the compliance matrix's first three rows.
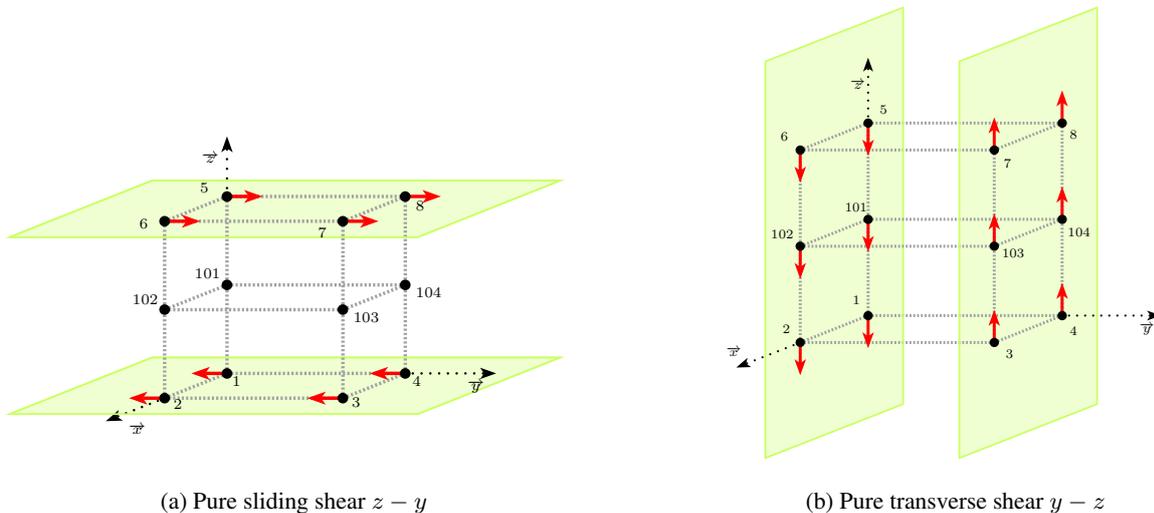
(a) Pure sliding shear $z - y$

(b) Pure transverse shear $y - z$

Figure 3: Pure shear schemes

Describing the deformed state $\gamma_{yz} = 2 \cdot \varepsilon_{yz}$, the simulation series is divided into two distinct schemes:

- the sliding shear scheme $z - y$ (method "**T1**") combines an enforced displacement δ_y along $-y$ on face $z = 0$, the same displacement δ_y along $+y$ on face $z = 1$, and constraints of plane contact on the same faces $z = 0$ and $z = 1$;

- the transverse shear scheme $y - z$ (method "**T2**") combines an enforced displacement δ_z along $-z$ on face $y = 0$, the same displacement δ_z along $+z$ on face $y = 1$, and constraints of plane contact on the same faces $y = 0$ and $y = 1$.

In both cases, the constraints of plane contact are necessary in order to generate pure shear. As for the previous simulations, computing the stress values σ_{ij} leads to the remaining constants of matrix S.

3   Validation

3.1   Homogeneous triclinic sample

The method "**T1**" has been first validated onto a simple, homogeneous case. For this example, a cuboid 8-node element whose dimensions are $L_x = 20\,\text{mm}$, $L_y = 40\,\text{mm}$ and $L_z = 60\,\text{mm}$ was used, to which a triclinic material defined by the elasticity matrix

$$C^{\text{exp}} = \begin{bmatrix} 3.51 & 0.47 & 1.27 & -0.67 & -0.02 & -0.56 \\ & 13.2 & 1.03 & -0.04 & -0.07 & 0.24 \\ & & 2.97 & -0.23 & -0.59 & 0.14 \\ & & & 0.37 & 0.17 & -0.07 \\ & \text{sym.} & & & 1.09 & 0.06 \\ & & & & & 0.81 \end{bmatrix} \cdot 10^9 \tag{5}$$

and the associated compliance matrix

$$S^{\text{exp}} = \begin{bmatrix} 0.926 & -0.016 & -0.397 & 1.848 & -0.538 & 0.913 \\ & 0.079 & -0.022 & -0.041 & 0.001 & -0.034 \\ & & 0.570 & -0.649 & 0.426 & -0.454 \\ & & & 6.719 & -1.483 & 2.093 \\ & \text{sym.} & & & 1.407 & -0.678 \\ & & & & & 2.186 \end{bmatrix} \cdot 10^{-9} \tag{6}$$

was applied, but without any preloading or friction conditions.

Each simulation has been made with enforced displacements of magnitude $\delta = 1\,\text{mm}$. A linear static solution is initiated (completed within a few seconds), including output requests at all nodes in terms of displacements and reaction forces. Computing the stress values from the reaction forces leads, for the deformed state ε_{xx}, to the first row of the equivalent compliance matrix:

$$\begin{Bmatrix} S_{11} \\ S_{12} \\ S_{13} \\ S_{14} \\ S_{15} \\ S_{16} \end{Bmatrix} = \begin{Bmatrix} 9.262 \cdot 10^{-10} \\ -1.582 \cdot 10^{-11} \\ -3.973 \cdot 10^{-10} \\ 1.848 \cdot 10^{-9} \\ -5.376 \cdot 10^{-10} \\ 9.133 \cdot 10^{-10} \end{Bmatrix} \tag{7}$$

The values found here are very close to the initial compliance matrix, including the terms of coupling between tension-compression and shear, namely S_{14}, S_{15} and S_{16}. The maximum relative discrepancy U_{max}^{rel} is such that

$$U_{max}^{\text{rel}} = \max_{i,j} \left| \frac{S_{ij} - S_{ij}^{\text{exp}}}{S_{ij}^{\text{exp}}} \right| = 0.8\% \,, \tag{8}$$

which is very low and therefore shows that the computed results are close to the initial values. The other rows are computed in the same way. As the values match, the validation is successful for this triclinic homogeneous element. Identical results are found with method "**T2**".

3.2 Preloaded homogeneous structure

3.2.1 Global structure

The second application of the methods is an analysis of a preloaded structure. The FE model is a homogeneous cuboid of isotropic steel (Young's modulus $E = 207\,\text{GPa}$, Poisson's ratio $\nu = 0.292$ and density $\rho = 7875\,\text{kg} \cdot \text{m}^{-3}$) of respective dimensions along x, y and z of 100 mm, 70 mm and 80 mm, and has 1,008 elements and 8,034 DOFs. Tension preloads are applied along direction y to the structure. The faces $y = 0\,\text{mm}$ and $y = 70\,\text{mm}$ are subjected to static forces of respective total magnitudes $9.81 \cdot 10^6\,\text{N}$ and $-9.81 \cdot 10^6\,\text{N}$, equally distributed on the faces' nodes, so that $\pm 81.1 \cdot 10^3\,\text{N}$ is applied along y to each of these nodes (the values have been chosen to be voluntarily high to ensure observing notable effects on the responses, and none of the yield or fracture limits are taken into account in the simulation: the material is assumed not to ever reach any of these limits while calculating the solutions). Also, a node-to-ground 3-D stiffness element is linked to each of the global cuboid's 8 outer nodes on every direction x, y and z. The initial structure is illustrated on Figure 4.

3.2.2 Equivalent material

To apply the identification method and determine an equivalent material, a sample is created from a few elements of the structure: 3 elements along y (48 DOFs), as shown on Figure 5. To recreate the stress field existing in the global structure, the sample's 8 outer nodes are subjected to the same nodal loads ($\pm 81.1 \cdot 10^3\,\text{N}$ per node), as the dimensions of the base cell are identical in the sample and in the global structure. To stabilise the system, a node-to-ground 3-D stiffness element is linked to each of the sample's 8 outer nodes on every direction x, y and z.

A 48×48 stiffness matrix is computed (which is real and symmetric) and takes into account the influence of the preload. By creating a new model with the sample's 16 nodes (and no elements), and importing the
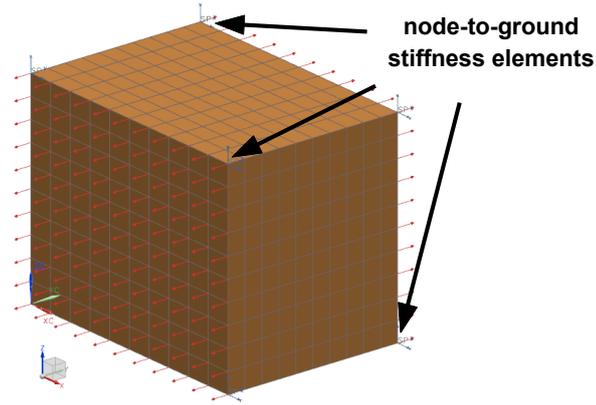
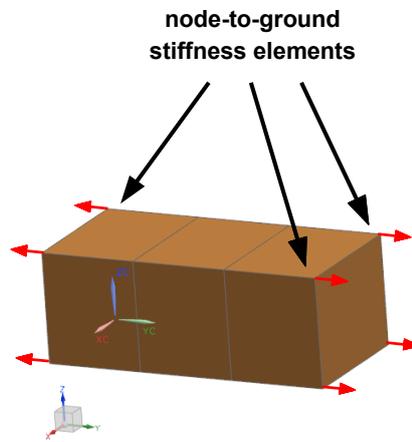Figure 4: Initial structure under preloading (thin red arrows)

Figure 5: Sample under preloading (red arrows)

stiffness matrix as an external superelement, a linear static solution is initiated to apply the methods "**T1**" and "**T2**" presented in Section 2. Post-processing the results yields the elasticity matrices

$$
C^{\text{ITL1}} = \begin{bmatrix}
265 & 118 & 110 & -4.82 \cdot 10^{-6} & -1.66 \cdot 10^{-5} & -1.89 \cdot 10^{-6} \\
 & 316 & 118 & -5.55 \cdot 10^{-6} & -1.69 \cdot 10^{-5} & 7.56 \cdot 10^{-6} \\
 & & 264 & -1.29 \cdot 10^{-5} & -4.43 \cdot 10^{-5} & 6.54 \cdot 10^{-6} \\
 & & & 51.2 & 8.27 \cdot 10^{-6} & 5.16 \cdot 10^{-4} \\
\text{sym.} & & & & 97.4 & 9.97 \cdot 10^{-1} \\
 & & & & & 182
\end{bmatrix} \cdot 10^9 \qquad (9)
$$

and

$$C^{\text{ITL2}} = \begin{bmatrix} 265 & 118 & 110 & -8.39 \cdot 10^{-6} & -1.32 \cdot 10^{-5} & -8.44 \cdot 10^{-7} \\ & 316 & 118 & -9.64 \cdot 10^{-6} & -1.35 \cdot 10^{-5} & 3.79 \cdot 10^{-6} \\ & & 264 & -2.24 \cdot 10^{-5} & -3.52 \cdot 10^{-5} & 3.43 \cdot 10^{-6} \\ & & & 88.9 & -2.20 \cdot 10^{-5} & -4.07 \cdot 10^{-8} \\ & \text{sym.} & & & 77.4 & 0.00 \\ & & & & & 89.1 \end{bmatrix} \cdot 10^9 , \tag{10}$$

respectively corresponding to "**T1**" and "**T2**" methods. Associated to them, the matrix corresponding to steel (without preloading) is detailed as following:

$$C^{\text{stl}} = \begin{bmatrix} 273 & 125 & 125 & 0 & 0 & 0 \\ & 273 & 125 & 0 & 0 & 0 \\ & & 273 & 0 & 0 & 0 \\ & & & 80.1 & 0 & 0 \\ & \text{sym.} & & & 80.1 & 0 \\ & & & & & 80.1 \end{bmatrix} \cdot 10^9 . \tag{11}$$

Judging from the values of the matrices, the following observations can be made:

- The terms of terms of coupling between tension-compression and shear are relatively low;

- In both matrices C^{ITL1} and C^{ITL2}, the tension preloading along y resulted in a significantly higher value of the coefficient C_{22} (diagonal term of Hooke's law in direction yy) compared to C^{stl}. This is consistent with the expected stiffening effect from tension preloading in this direction [12].

Two equivalent homogeneous structures are then computed, with the same dimensions and the same density as the initial model, and in which the equivalent stiffness values of every node-to-ground elements have taken into account the stiffening effects.

3.2.3 Correlation analysis

To evaluate the validity of the equivalent materials to recreate the behaviour of the preloaded structure, a state of modal correlation is calculated. To perform this, modal bases of the first 200 modes (excluding the 6 low-frequency modes describing the "suspension" related to the node-to-ground elements) are computed for the following structures:

- **Init** (initial structure made of homogeneous steel);

- **Prld** (initial structure with preloading);

- **T1** (equivalent structure with material identified with "**T1**" method);

- **T2** (equivalent structure with material identified with "**T2**" method).

The similarities in the modal behaviours of two structures can be evaluated by a process of correlation. In this paper, this correlation is evaluated by comparing the natural frequencies and the deformed shapes of the models by computing the matrices $[\Delta f]$ and $[MAC]$. Each component $\Delta f\left(m_{e,i}, m_{a,j}\right)$ of the matrix $[\Delta f]$

expresses the relative difference between the natural frequency of the first structure's i-th mode $m_{1,i}$ and the second structure's j-th mode $m_{2,j}$, and is defined by the relation:

$$\Delta f\left(m_{1,i}, m_{2,j}\right) = \frac{f_{1,i} - f_{2,j}}{f_{1,i}} \ , \tag{12}$$

where $f_{1,i}$ et $f_{2,j}$ are the natural frequencies respectively corresponding to the modes $m_{1,i}$ and $m_{2,j}$. The second matrix, $[MAC]$, expresses the similarities between the deformed shapes of the modes $m_{1,i}$ and $m_{2,j}$ (respectively called $\{\phi_{1,i}\}$ and $\{\phi_{2,j}\}$), according to the so-called MAC criterion (*Modal Assurance Criterion*). Its components $MAC\left(m_{1,i}, m_{2,j}\right)$ are defined by the expression [13]:

$$MAC\left(m_{1,i}, m_{2,j}\right) = \frac{\left|\{\phi_{1,i}\}^{\mathsf{T}}\{\phi_{2,j}\}\right|^2}{\{\phi_{1,i}\}^{\mathsf{T}}\{\phi_{1,i}\}\{\phi_{2,j}\}^{\mathsf{T}}\{\phi_{2,j}\}} \ . \tag{13}$$

According to these expressions, two models perfectly correlated are defined by a matrix $[\Delta f]$ in which every diagonal component is at 0%, and a matrix $[MAC]$ in which every diagonal is at 100%, and the others at 0%. Finally, the pairs of modes for which MAC values are highest are assembled, and are taken into account for the correlation if the MAC values are above a fixed threshold.

For the correlation, the reference modal basis is "**PrId**", to which the other bases are compared. The MAC-threshold is fixed at 0% for pairing the modes (so that all the modes are paired and taken into account). The results of the correlation are gathered in Table 1. For N_{pm} mode pairs in a given correlation, the entities $\overline{|\Delta f|}$ and $\overline{MAC}$ are defined by the expressions:

$$\overline{|\Delta f|} = \frac{1}{N_{pm}} \cdot \sum_{q=1}^{N_{pm}} |\Delta f\left(m_1^q, m_2^q\right)| \tag{14}$$

and

$$\overline{MAC} = \frac{1}{N_{pm}} \cdot \sum_{q=1}^{N_{pm}} MAC\left(m_1^q, m_2^q\right) \ , \tag{15}$$

where m_1^q and m_2^q are the modes composing the q-th pair.

	Init	T1 (sliding shear)	T2 (transverse shear)
$\overline{|\Delta f|}$ [%]	3.85	7.64	1.40
$\overline{MAC}$ [%]	72.0	42.6	90.3

Table 1: Correlation of the first 194 modes above 3,000 Hz

Table 1 clearly shows that method "**T2**" is capable of recreating the behaviour of the structure under preloads with good accuracy, while method "**T1**" is much less efficient in this setting.

3.3 Preloaded laminated structure

3.3.1 Global structure

For the last validation case, a laminated cuboid of 5,024 elements, 30,144 DOFs and respective dimensions along x, y and z of 210 mm, 110 mm and 60 mm is analysed. The stack's base cell is composed of 3 isotropic layers, the properties of which are detailed in Table 2, and is oriented along z. For each layer, E is the Young's modulus, ν the Poisson's ratio, ρ the density and e the thickness. Also, the volume fraction ϕ_n of layer n is defined by the layer's volume V_n and the base cell's total volume V^{cell}, so that

$$V^{\text{cell}} = \sum_{n=1}^{3} V_n \tag{16}$$

and

$$\phi_n = \frac{V_n}{V^{\text{cell}}} \ . \tag{17}$$

	Steel	Polypropylene	Titanium
E [GPa]	207	2.0	121
ν [$-$]	0.25	0.40	0.34
ρ $\left[\text{kg} \cdot \text{m}^{-3}\right]$	7875	1200	4430
e [cm]	0.40	0.20	0.40
ϕ [$-$]	0.40	0.20	0.40

Table 2: Details of the layers

In this case, the structure is subjected to tension preloads along the stacking direction (z). The total loads on the top and bottom faces are respectively $13.2 \cdot 10^9$ N and $-13.2 \cdot 10^9$ N, equally distributed on the faces' nodes, so that $\pm 500 \cdot 10^3$ N is applied along z to each of these nodes. As before, the values have been chosen to be voluntarily high to ensure observing notable effects on the responses. None of the yield or fracture limits are taken into account in the simulation: the material is assumed not to ever reach any of these limits while calculating the solutions. Also, no contact conditions are taken into account between the different layers: the structure is assumed to experience no delamination.

A node-to-ground 3-D stiffness element is linked to each of the global cuboid's 8 outer nodes on every direction x, y and z. The global structure taken as reference is illustrated on Figure 6.

3.3.2 Equivalent material

To apply the identification method and determine an equivalent material, a sample is created from a few elements of the structure. In this application, the sample consists of the 3-layered base cell (48 DOFs) which constitutes the entire model, and is illustrated on Figure 7. To recreate the stress field existing in the global structure, the sample's outer nodes are subjected to the same nodal loads ($\pm 500 \cdot 10^3$ N per node), as the dimensions of the base cell are identical in the sample and in the global structure. To stabilise the system, a
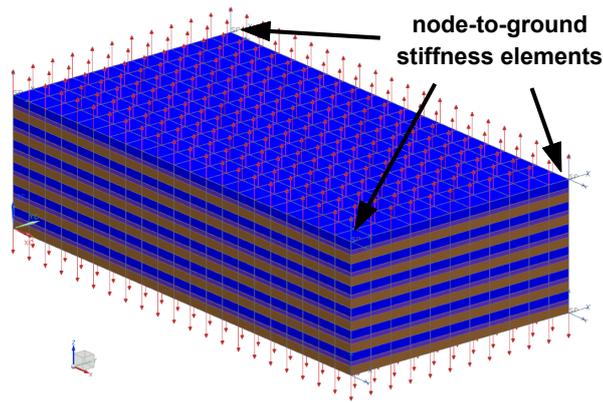
Figure 6: Global laminated structure under preloading (thin red arrows)

node-to-ground 3-D stiffness element is linked to each of the sample's 8 outer nodes on every direction x, y and z.
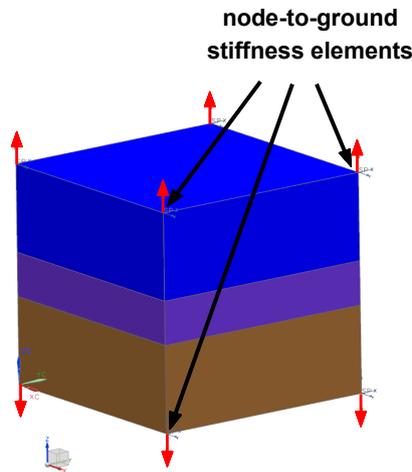

Figure 7: Base cell under preloading (red arrows)

As before, the addition of node-to-ground elements to the sample is necessary to stabilise the system, and yet independent from the initial, global structure. Again, the stiffness values of the node-to-ground elements are negligible in comparison to the sample's stiffness matrix's.

A 48×48 stiffness matrix is computed (which is real and symmetric) and takes into account the influence of the preload. By creating a new model with the sample's 16 nodes (and no elements), and importing the stiffness matrix as an external superelement, a linear static solution is initiated to apply the methods "**T1**" and "**T2**" presented in Section 2. Post-processing the results yields the elasticity matrices

$$C^{\mathrm{LTL1}} = \begin{bmatrix} 146 & 52.2 & 36.1 & -2.16 & -2.03 & -0.207 \\ & 146 & 36.1 & -2.16 & -2.03 & -0.207 \\ & & 110 & -6.61 & -6.21 & -0.635 \\ & & & 30.2 & 0.416 & 1.68 \\ & \text{sym.} & & & 30.1 & 1.33 \\ & & & & & 47.6 \end{bmatrix} \cdot 10^9 \tag{18}$$

and

$$C^{\text{LTL2}} = \begin{bmatrix} 147 & 52.6 & 37.2 & -4.89 & -4.60 & -1.02 \\ & 147 & 37.2 & -4.89 & -4.60 & -1.02 \\ & & 114 & -15.0 & -14.1 & -3.14 \\ & & & 66.5 & 2.87 & 7.65 \\ & \text{sym.} & & & 66.2 & 7.28 \\ & & & & & 49.1 \end{bmatrix} \cdot 10^9 \ , \tag{19}$$

respectively corresponding to "**T1**" and "**T2**" methods.

Judging from the values of the matrices, several observations can be made:

- Non-negligible terms of coupling between tension-compression and shear have been determined for both materials;

- In both matrices C^{LTL1} and C^{LTL2}, the directions x and y have similar coefficients, which shows that the laminated structure has in this case an equivalent behaviour in planes normal to the stacking direction;

- In C^{LTL2} (transverse shear), the absolute values involving shear in directions yz and xz are significantly greater than in C^{LTL1} (sliding shear).

The homogeneous structure to which the equivalent material of each method is applied has the same dimensions and the same total mass as the reference cuboid, and is made of 1-centimetre-long cubic, 8-node, solid elements. Therefore, the equivalent homogeneous material's density ρ^{hmg} is calculated by the relation of weighted average:

$$\rho^{\text{hmg}} = \sum_{n=1}^{N} \rho_n \phi_n \ , \tag{20}$$

where ρ_n is the density of each layer n.

Two equivalent homogeneous structures are then created, with the same dimensions as the initial model. For each of them, the dimensions are identical to the reference matrix's, but one-centimetre-long cubic elements replace the three-layered base-cells that were homogenised. Also, the equivalent stiffness values of every node-to-ground elements (in the equivalent homogeneous FE models) have taken into account the stiffening effects.

3.3.3 Correlation analysis

To evaluate the validity of the equivalent materials to recreate the behaviour of the preloaded structure, a state of modal correlation is calculated. To perform this, modal bases of the first 50 modes (excluding the 6 low-frequency modes describing the "suspension" related to the node-to-ground elements) are computed for the following structures:

- **Init** (initial laminated structure made isotropic layers);

- **Prld** (initial structure with preloading);

- **T1** (equivalent structure with material identified with "**T1**" method);

- **T2** (equivalent structure with material identified with "**T2**" method).

	Init	T1 (sliding shear)	T2 (transverse shear)
Nb paired modes	23	36	17
$\overline{\lvert \Delta f \rvert}$ [%]	38.0	12.1	14.7
$\overline{MAC}$ [%]	90.3	87.5	88.1

Table 3: Correlation of the first 44 modes above 2,500 Hz

For the correlation, the reference modal basis is "**PrId**", to which the other bases are compared. The paired modes for which MAC values are below 70% are discarded. The results of the correlation are gathered in Table 3, where $\overline{\lvert \Delta f \rvert}$ and $\overline{MAC}$ are computed from the paired modes with the expressions (14) and (15).

Table 3 clearly shows that in spite of the important behaviour difference induced by the application of the preloads, method "**T1**" is capable of identifying 36 modes over 44. However, the material from method "**T2**" is not efficient to simulate the behaviour of the initial structure under preloading, as only 17 modes over 44 are identified.

Therefore, it can be expressed that recreating the lower-frequency modes of laminated structures with homogeneous equivalent materials requires identifying the elastic properties with sliding shear simulations instead of transverse shear. At the contrary, the results of the analysis in Subsection 3.2 showed that identifying an equivalent material for a continuous anisotropic structure is much more accurate with transverse shear simulations.

4   Conclusion

In this paper, a novel method for identifying equivalent materials to anisotropic structures was proposed. It has been shown that the method is also able to identify equivalent elasticity matrices for structures subjected to external conditions, and its validity has been ascertained with various applications on structures subjected to preloading. The two distinctive approaches to analyse shear have been compared; sliding shear identification schemes are more appropriate to describe laminated structures, whereas transverse shear are the most accurate to simulate the behaviour of an anisotropic continuous model. Additionally, this identification method can be applied to superelements, unlike existing homogenization techniques, and can therefore convert stiffness matrices into equivalent elasticity matrices.

APPENDIX: Node sets in the case of a structure with two layers

The node sets $\mathcal{U}_{x0}, \mathcal{U}_{x1}, \mathcal{U}_{y0}, \mathcal{U}_{y1}, \mathcal{U}_{z0}$ and $\mathcal{U}_{z1}$ are defined for the development of the identification method (cf. Figure 2) with a structure composed of two separated 8-node solid elements. The details of these node sets are given in Table 4.

node set	face	nodes
$\mathcal{U}_{x0}$	$x = 0$	1, 2, 5, 6, 101, 102
$\mathcal{U}_{x1}$	$x = 1$	3, 4, 7, 8, 103, 104
$\mathcal{U}_{y0}$	$y = 0$	1, 4, 5, 8, 101, 104
$\mathcal{U}_{y1}$	$y = 1$	2, 3, 6, 7, 102, 103
$\mathcal{U}_{z0}$	$z = 0$	1, 2, 3, 4
$\mathcal{U}_{z1}$	$z = 1$	5, 6, 7, 8

Table 4: Details about node set names in the case of a 8-outer-node structure with two layers

References

[1] A. L. Kalamkarov, I. V. Andrianov, and V. V. Danishevs'kyy, "Asymptotic homogenization of composite materials and structures," *Applied Mechanics Reviews*, vol. 62, 2009.

[2] J.-M. Berthelot, *Composite materials, mechanical behavior and structural analysis.* Springer, 1999.

[3] Y. Chevalier and J. V. Tuong, *Mechanics of viscoelastic materials and wave dispersion.* Iste/Wiley, 2010.

[4] D. Begis, G. Duvaut, and A. Hassim, "Homogénéisation par éléments finis des modules de comportements élastiques de matériaux composites," Institut National de Recherche en Informatique et Automatique, Tech. Rep. 101, 1981.

[5] P. Alart and F. Lebon, "Numerical study of a stratified composite coupling homogenization and frictional contact," *Mathematical and computer modelling*, vol. 28, no. 4, pp. 273–286, 1998.

[6] G. Peillex, L. Baillet, and Y. Berthier, "Homogenization in non-linear dynamics due to frictional contact," *International Journal of Solids and Structures*, vol. 45, no. 9, pp. 2451–2469, 2008.

[7] J. Yvonnet, D. Gonzalez, and Q.-C. He, "Numerically explicit potentials for the homogenization of nonlinear elastic heterogeneous materials," *Computer Methods in Applied Mechanics and Engineering*, vol. 198, no. 33, pp. 2723–2737, 2009.

[8] M. Pirnat, G. Čepon, and M. Boltežar, "Introduction of the linear contact model in the dynamic model of laminated structure dynamics - an experimental and numerical identification," *Mechanism and Machine Theory*, vol. 64, pp. 144–154, 2013.

[9] D. Begis, A. Bestagno, G. Duvaut, A. Hassim, and M. Nuc, "A new method of computing global elastic moduli for composite materials," Institut National de Recherche en Informatique et Automatique, Tech. Rep. 195, 1983.

[10] Y. Chevalier, *Comportements élastique et viscoélastique des composites.* Techniques de l'Ingénieur, 1988, vol. 5.

[11] L. Gornet, *Généralités sur les matériaux composites*, 2008.

[12] R. D. Blevins, *Formulas for natural frequency and mode shape.* Van Nostrand Reinhold New York, 1979.

[13] D. J. Nefske and S. H. Sung, "Correlation of a coarse-mesh finite element model using structural system identification and a frequency response assurance criterion," in *Proceedings of the International Modal Analysis Conference*, 1996, pp. 597–602.